Magnetic and Spectroscopic Characterization of an Iron Porphyrin Peroxide Complex. Peroxoferrioctaethylporphyrin(1-)

Judith N. Burstyn,[†] James A. Roe,[†] Andrew R. Miksztal,[†] Ben A. Shaevitz,[‡] George Lang,[‡] and Joan Selverstone Valentine*[†]

Contribution from the Department of Chemistry and Biochemistry and Molecular Biology Institute, University of California, Los Angeles, Los Angeles, California 90024, and Department of Physics, Davey Laboratory, The Pennsylvania State University, University Park, Pennsylvania 16802. *Received April 16, 1987*

Abstract: A ferric porphyrin peroxide complex, which is possibly analogous to an oxygenated intermediate involved in reactions of cytochrome P450, has been isolated and characterized. The tetramethylammonium salt of peroxoferrioctaethylporphyrin, $[Me_4N][Fe(OEP)O_2]$, was prepared by the reaction of $Fe^{III}(OEP)Cl$ with 2 equiv of tetramethylammonium superoxide in acetonitrile and isolated by cooling to -30 °C. An elemental analysis of the microcrystalline solid was consistent with the formulation above. Magnetic susceptibility measurements on the solid material gave a value of 5.75 μ_B for the effective magnetic moment, confirming the high-spin ferric state of the iron atom in this complex. Mössbauer spectra, which exhibited an isomer shift of +0.67 mm/s, and ESR spectra, with g values of 4.2 and 9.5, were also consistent with a high-spin ferric iron. The data from the Mössbauer, magnetic susceptibility, and powder ESR measurements were successfully simulated by a rhombic spin Hamiltonian. The magnitude of D was determined to be approximately 0.85 cm^{-1} with $\lambda = E/D = 0.29$, close to the rhombic limit of 0.33. On the basis of these data, the energy difference between the two lowest Kramers' doublets is approximated at 2.9 cm^{-1}.

There is considerable interest in the characterization of iron porphyrin complexes containing reduced forms of dioxygen as potential analogues of intermediates in the activation of dioxygen by heme-containing oxygenase and peroxidase enzymes. It is hoped that such complexes will be useful in the elucidation of the mechanism by which the oxygen–oxygen bond is cleaved to generate the high-valent iron oxo species believed to be the active oxidizing species in cytochrome P450. Recent studies have focused on metal peroxide complexes as possible precursors to this active oxidant.[1,2]

The identification of the ferric porphyrin peroxide complex, $Fe(TPP)O_2^-$,[3] was originally reported by Valentine and co-workers in 1978.[4] This complex was obtained in dimethyl sulfoxide (DMSO) solution by the reaction of ferric porphyrins with 2 equiv of superoxide or by the reaction of ferrous porphyrins with 1 equiv of superoxide, forming the new species by reaction 1.[4,5] The

$$PFe^{III}Cl \xrightarrow{O_2^-} PFe^{II} \xrightarrow{O_2^-} [PFe^{III}(O_2^{2-})]^- \qquad (1)$$

complex thus formed had been observed previously[6] but was thought to be a ferrous superoxide complex, in part because of the pronounced red shift of the Soret absorbance in the visible spectrum. The presence of an electron spin resonance (ESR) signal at $g = 4.2$, characteristic of rhombic high-spin iron(III), and the similarity of this reaction to the reaction of iron(II) ethylenediaminetetraacetate with superoxide to form a ferric peroxide complex[7] led to the postulate by McCandlish and Valentine that the product of the reaction of ferrous porphyrins with superoxide was a ferric porphyrin peroxide complex.[4] The frequency of the oxygen–oxygen stretching vibration in the infrared spectrum of $Fe(OEP)O_2^-$ was identified ($\nu_{O-O} = 806$ cm^{-1}) and shown to shift on isotopic substitution with $^{18}O_2^-$ ($\nu_{O-O} = 759$ cm^{-1}).[5] The position of this vibration was within the region characteristic of bound peroxide. Welborn et al.[8] subsequently showed that $Fe(OEP)O_2^-$ could also be prepared by electrochemical reduction of the ferrous dioxygen complex, as shown in reaction 2. The

$$PFe^{II} \xrightarrow{O_2} PFeO_2 \xrightarrow{e^-} PFe^{III}O_2^- \qquad (2)$$

Fe(III) oxidation state of these iron peroxo porphyrin complexes was confirmed by the measurement of the magnetic susceptibility of $Fe(TPP)O_2^-$ in solution by the Evans method ($N_{eff} \geq 5.6$ μ_B).[9] Solid-state characterization of the iron porphyrin peroxide complex has been hampered by its instability. Reed prepared solid samples by the reaction of an iron(I) porphyrin with dioxygen in tetrahydrofuran (THF) followed by removal of the solvent.[10] Mössbauer data collected on this solid again confirmed the high-spin ferric state of the iron atom, although detailed interpretation of these spectra was not possible due to the presence of large amounts of contaminants.[11] Other workers have attempted to characterize $Fe(OEP)O_2^-$ in the solid state by ESR and Mössbauer spectroscopy, but the purity of their material was never determined.[12] Recently, a structural study of this complex by EXAFS (extended X-ray absorption fine structure) spectroscopy has been reported. Friant et al.[13] prepared the complex $[Na(THF)_3][Fe(TPP)O_2]$ by oxygenation of $[Na(THF)_3][Fe^I(TPP)]$ in the solid state in a manner similar to that used by Reed.[10] On the basis of a difference analysis of their EXAFS data, wherein the contribution of the porphyrin was removed, the

[†] University of California, Los Angeles.
[‡] The Pennsylvania State University.

(1) Groves, J. T.; Watanabe, Y. *J. Am. Chem. Soc.* **1986**, *108*, 7834–7836.
(2) Groves, J. T.; Watanabe, Y.; McMurry, T. J. *J. Am. Chem. Soc.* **1983**, *105*, 4489–4490.
(3) Abbreviations used in text: OEP, octaethylporphyrin dianion; TPP, tetraphenylporphyrin dianion; Me, methyl (CH_3); ESR, electron spin resonance; μ_B, Bohr magneton; K222, 4,7,13,16,21,24-hexaoxo-1,10-diazabicyclo[8.8.8]hexacosane; SQUID, superconducting quantum inteference device; K18-C-6, potassium 18-crown-6.
(4) Valentine, J. S.; McCandlish, E. In *Frontiers of Biological Energetics: Electrons to Tissues*; Dutton, P. L., Leigh, J. S., Scarpa, A., Eds.; Academic: New York, 1978; Vol. 2, pp 933–939.
(5) McCandlish, E.; Miksztal, A. R.; Nappa, M.; Sprenger, A. Q.; Valentine, J. S.; Stong, J. D.; Spiro, T. G. *J. Am. Chem. Soc.* **1980**, *102*, 4268–4271.
(6) Koltover, V. K.; Koifman, O. I.; Khenkin, A. M.; Shteinman, A. A. *Izv. Akad. Nauk SSSR, Ser. Khim.* **1978**, *7*, 1690–1691.
(7) McClune, G. J.; Fee, J. A.; McClusky, G. A.; Groves, J. T. *J. Am. Chem. Soc.* **1977**, *99*, 5220–5222.
(8) Welborn, C. H.; Dolphin, D.; James, B. R. *J. Am. Chem. Soc.* **1981**, *103*, 2869–2871.
(9) Shirazi, A.; Goff, H. M. *J. Am. Chem. Soc.* **1982**, *104*, 6318–6322.
(10) Reed, C. A. In *Electrochemical and Spectrochemical Studies of Biological Redox Compounds*; Kadish, K. M., Ed.; Advances in Chemistry 201; American Chemical Society: Washington, DC, 1982; pp 333–356.
(11) Reed, C. A., Personal communication.
(12) Khenkin, A. M.; Shteinman, A. A. *Kinet. Katal.* **1982**, *23*, 219–222; English translation, pp 185–187.
(13) Friant, P.; Goulon, J.; Fischer, J.; Ricard, L.; Schappacher, M.; Weiss, R.; Momenteau, M. *Nouv. J. Chim.* **1985**, *9*, 33–40.

0002-7863/88/1510-1382$01.50/0

authors concluded that the peroxide ligand was symmetrically bonded to the iron at a distance of 1.80 Å and that that iron atom was slightly (>0.3 Å) displaced from the plane of the four nitrogen atoms.

We report here the isolation of the ferric porphyrin peroxide complex, $[Me_4N][Fe(OEP)O_2]$, as a microcrystalline solid, from the reaction of Fe(OEP)Cl with tetramethylammonium superoxide. We have characterized this solid material by a variety of methods including electron spin resonance and Mössbauer spectroscopies and measurement of its magnetic susceptibility.

Experimental Section

General Procedures. All operations involving the synthesis and isolation of $[Me_4N][Fe(OEP)O_2]$ were carried out in a Vacuum Atmospheres glovebox under a helium atmosphere. Acetonitrile (CH_3CN) was distilled from calcium hydride (CaH_2) and then passed through Woehlm Super I activity grade alumina. This solvent was then stirred for 1 h with finely ground potassium superoxide to ensure complete removal of water and filtered by passage through more alumina. The absence of an electron spin resonance signal demonstrated that the solvent contained no dissolved superoxide. Tetramethylammonium superoxide (Me_4NO_2) was prepared by a published procedure,[14] and its purity was determined by titration to be 95% or better.[15] Potassium superoxide (KO_2, Alfa) was finely ground prior to use. Kryptofix 222 (K222, MCB) was purified by drying over phosphorus pentoxide (P_2O_5), followed by recrystallization from dry heptane inside the glovebox and vacuum distillation [175 °C (5×10^{-3} Torr)]. Iron(III) octaethylporphyrin chloride (Fe(OEP)Cl) was purchased from Mid-Century Chemical and dried at 80 °C in vacuo. Devcon 5-Minute Epoxy was used to embed the samples for magnetic susceptibility and Mössbauer spectroscopy and to seal ESR tubes.

Synthesis of $[Me_4N][Fe(OEP)O_2]$. Fe(OEP)Cl (40 mg) and Me_4NO_2 (16 mg, 2.2 equiv) were suspended in dry acetonitrile (16 mL) and stirred vigorously for no more than 2 min. The resulting blood red solution was filtered through a solvent-resistant disposable filter and placed in the glovebox freezer (−30 °C) overnight. The polycrystalline solid was isolated by filtration and washed rapidly with the cold mother liquor to yield 15.1 mg (40%) of $[Me_4N][Fe(OEP)O_2]$. The solid could be stored in the drybox at −30 °C for several weeks without significant decomposition, as evidenced by the visible spectrum of the redissolved solid. When exposed to air, the solid decomposed to produce the (μ-oxo)ferric porphyrin dimer. Samples for elemental analysis were sent in sealed containers under an argon atmosphere to Galbraith Laboratories, Knoxville, TN. Anal. Calcd for $C_{40}H_{56}FeN_5O_2$: C, 69.15; H, 8.12; N, 10.08. Found: C, 68.26; H, 7.27; N, 10.13.

Electron Spin Resonance Spectroscopy. Electron spin resonance spectra were measured on an IBM (Bruker) 200D spectrometer equipped with an Oxford Instruments liquid helium cryostat. The field was measured with an NMR gaussmeter and the frequency calibrated with a digital counter. The g values were determined by measuring the field at the maximum, minimum, or zero crossing point of the derivative signal. Solid samples of 1–3 mg of $Fe(OEP)O_2^-$ were prepared in the drybox, powdered, and sealed in an ESR tube with epoxy. The temperature dependence of the intensity of the $g = 4.2$ resonance was studied between 3.8 and 20 K, and the resulting data were simulated on an Apple II+ computer, by a computational routine called FERSIM, which was written in Basic by J.A.R.

Mössbauer Spectroscopy. Due to the air and moisture sensitivity of the complex, samples for natural-abundance Mössbauer spectroscopy were prepared by embedding the solid iron peroxo complex, $[Me_4N][Fe(OEP)O_2]$ (81 and 90 mg), in epoxy disks, which were then stored at liquid nitrogen temperature until they were used. A disk of pure epoxy, prepared with equal masses of resin and hardener, absorbed only 10% of the 14.4-keV radiation. The Mössbauer spectra were recorded in horizontal transmission geometry by a constant-acceleration spectrometer operated in connection with a 256 channel analyzer in the time scale mode.[16] The source of radiation was ^{57}Co diffused in a rhodium foil matrix and was kept at room temperature at all times. Calibrations of the spectrometer were made with iron foil at room temperature, and the centroid of its Mössbauer spectrum was taken as the zero of velocity for all reported data. Spectra recorded in a high magnetic field were obtained by a split coil superconducting magnet with the γ-beam directed normal to the field.

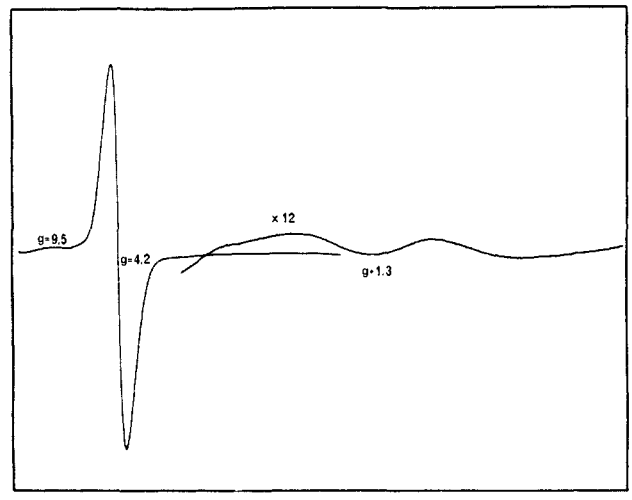

Figure 1. Solid-state ESR spectrum of $[Me_4N][Fe(OEP)O_2]$ recorded at 10.0 K on a finely powdered sample: microwave frequency, 9.4416 GHz; modulation amplitude, 5 ΔG_{pp}; time constant, 100 ms; sweep width, 10000 G.

Magnetic Susceptibility Measurements. The measurement of solid-state susceptibilities was made on three samples of $[Me_4N][Fe(OEP)O_2]$ varying in size from 14.80 to 30.05 mg. The solid sample was carefully weighed into a Teflon mold, mixed with a known amount of epoxy (prepared from equal masses of hardener and resin), and allowed to set for 10 min inside the drybox. Once the plug had solidified, it was removed from the drybox and encased in a piece of shrink tubing. Control samples of both the shrink tube and a pure epoxy plug in shrink tube were run, and the temperature dependence of their gram susceptibilities was used to make a diamagnetic correction to the sample data. The susceptibility measurements were made on an SHE SQUID susceptometer at 2 and 10 kG between 2 and 300 K. A correction of -535×10^{-6} emu/mol was applied to the sample data to account for the diamagnetism of the porphyrin ligand, the iron atom, and the tetramethylammonium cation.[17,18] Theoretical curves were simulated for comparison with the data on an IBM personal computer.

Visible and Infrared Spectra. Optical absorption spectra were recorded on a Beckman 5270 spectrophotometer in 0.1-mm or 1.0-cm cells equipped with either septums or stopcocks to allow manipulations under inert atmosphere. Infrared spectra were taken on a Beckman 4260 or on a Perkin-Elmer 283, either as Nujol mulls between potassium bromide plates sealed with stopcock grease or as DMSO solutions in demountable cells with NaCl windows.

Results

Electron Spin Resonance Spectroscopy. The high degree of rhombicity of the iron center in $[Me_4N][Fe(OEP)O_2]$ is demonstrated by the presence of the intense signal at $g = 4.2$,[19] both in solution and as a powdered solid, as shown in Figure 1. In the solid-state spectra, a shoulder was observed on the large $g = 4.2$ signal at approximately $g = 9.5$. A weak transition was also observed in the region below $g = 2$, near $g = 1.3$, but its position was not well-defined due to its low intensity and large line width. Although a highly rhombic system is expected to have a transition below $g = 2$, which arises from the lowest doublet,[19] the small measured zero-field splitting in this complex implies that the intensity of this transition will be low even at 3.8 K.

The presence of the single broad resonance at $g = 4.2$ precluded the determination of the exact value of the rhombicity parameter, λ. When the method of Wickman, Klein, and Shirley was used,[20]

(14) Sawyer, D. T.; Calderwood, T. S.; Yamaguchi, K.; Angelis, C. T. *Inorg. Chem.* **1983**, *22*, 2577–2583.
(15) Kolthoff, I. M., Sandell, E. B., Meehan, E. J., Brukenstein, S., Eds. *Quantitative Chemical Analysis*; Macmillan: New York, 1969; pp 842–860.
(16) Lang, G. In *Applications of Mössbauer Spectroscopy*; Cohen, R. L., Ed.; Academic: New York, 1976; Vol. 1, pp 129–140.
(17) The value -470×10^{-6} emu/mol for the diamagnetic correction of OEP from: Scheidt, W. R.; Geiger, D. K.; Haller, K. J. *J. Am. Chem. Soc.* **1982**, *104*, 495–499.
(18) The diamagnetic correction for individual atoms from: *Theory and Applications of Molecular Paramagnetism*; Beaudreaux, E. A.; Mulray, L. N., Eds.; Wiley: New York, 1976; p 491.
(19) Blumberg, W. E. In *Magnetic Resonance in Biological Systems*; Ehrenberg, A., Malmstrom, B. G., Vanngard, T., Eds.; Pergamon: Oxford, 1966; pp 119–133.
(20) Wickham, H. H.; Klein, M. P.; Shirley, D. A. *J. Chem. Phys.* **1965**, *42*, 2113–2117.

Table I. Comparison of Experimental g Values and Those Calculated as a Function of the Rhombicity, E/D[a]

	experimental g values	calculated g values for E/D				
		0.23	0.25	0.27	0.29	0.33
lower doublet	9.5 ± 0.5	9.3	9.4	9.49	9.56	9.86
	~1.3	1.65	1.45	1.28	1.13	0.86
middle doublet	4.6 ± 0.06 max	4.88	4.76	4.64	4.53	4.28
	3.8 ± 0.06 min	3.61	3.76	3.90	4.03	4.28
	4.2 ± 0.06 inflectn	3.96	4.08	4.18	4.24	4.28
upper doublet	(9.5)	9.87	9.84	9.81	9.17	9.68

[a] The positions of the ESR transitions were calculated from the spin Hamiltonian described in the Discussion. The value of D was assumed to be greater than zero for these calculations. The errors in the experimentally determined g values reflect the average deviation of the maximum, minimum, or inflection point, measured in gauss, for three separate samples.

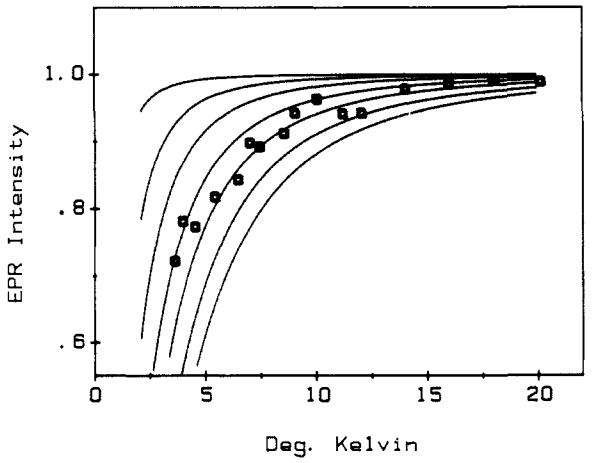

Figure 2. Intensity of the $g = 4.2$ signal as a function of temperature. The experimental data, obtained from a finely powdered solid sample, appear as circles. The solid curves are the calculated intensities for $\lambda = 0.29$. The lowest curve is for $D = 1.4$ cm^{-1}, and the uppermost curve is for $D = 0.2$ cm^{-1}, with the intervening curves being increments of 0.2. For these calculations D is assumed to be positive.

however, it was possible to estimate limits on the value of λ. A reasonable estimate of the principal g values associated with the middle doublet may be obtained by using the minimum, maximum, and inflection points of the $g = 4.2$ ESR absorption derivative as limits for the g values. A lower limit of λ may then be calculated from these estimates. The g values for the maximum, minimum, and inflection points of the main signal at $g = 4.2$ were compared to the calculated values derived from the rhombic spin Hamiltonian as a function of λ. The results of this analysis are given in Table I. The position and line width of this signal were consistent with $\lambda \geq 0.26$. The approximate position of both the upfield and downfield signals are consistent with this conclusion.

An estimate of the magnitude of the zero-field splitting parameter, D, was obtained by an analysis of the temperature dependence of the intensity of the $g = 4.2$ signal between 3.8 and 20 K. In the absence of a measured integrated intensity, the relative intensity was calculated on the basis of the peak-to-peak intensity times the square of the peak-to-peak field width. There was negligible change in the applied field and frequency during the course of the experiment. The change in the line width of the signal, measured from the difference in field between the maximum and minimum of the derivative signal, was also minimal. The contribution made by the Zeeman splitting to the temperature-dependent intensity was factored out by multiplying the calculated intensity by kT to leave only that fraction of the intensity related to the zero-field splitting. The corrected relative intensity of the $g = 4.2$ signal as a function of temperature is shown in Figure 2. The data were fit to a model in which this signal arises from the middle doublet in a system of three Kramers' doublets where the population of the middle doublet, and hence the relative intensity, is calculated by a Boltzmann distribution as described by eq 3. The energy differences in eq 3 refer to the

$$I_{rel} = A / 1 + e^{\Delta E_{12}/kT} + e^{-\Delta E_{23}/kT} \quad (3)$$

separation between the lowest and middle doublet (ΔE_{12}) and the middle and upper doublet (ΔE_{23}) in a three Kramers' doublet system. The factor A is an arbitrary constant used to normalize the data.

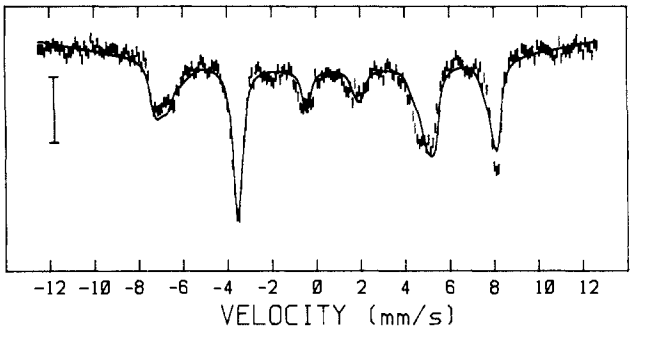

Figure 3. Mössbauer spectrum of $[Me_4N][Fe(OEP)O_2]$ measured at 4.2 K in a 60-kG applied field. The solid line is a calculation in the fast relaxation limit based on a $S = {}^5/_2$ spin Hamiltonian with $D = 0.85$ cm^{-1}, $\lambda = 0.29$, $-A/g_n\beta_n = 233.4$ kG/unit spin, $\delta = 0.67$ mm/s, $\Delta E_q = +0.62$ mm/s, line width $\Gamma = 0.42$ mm/s, and $\eta = 0.87$. The vertical bar represents 1% absorption.

The position of the major resonance indicates that $[Me_4N][Fe(OEP)O_2]$ is a rhombic high-spin iron system. The change in the intensity of this signal as a function of temperature has been successfully simulated, from which we conclude that the electronic structure of this complex is consistent with the presence of three closely spaced Kramers' doublets. The prominent signal at $g = 4.2$ arises from the middle doublet, while the weaker signal at $g = 9.5$ results from the overlap of the signals from the upper and lower doublets.[21] The best simulation of the signal intensity of the $g = 4.2$ resonance as a function of temperature was obtained for an energy difference of 2.9 cm^{-1} between the lowest doublets, when λ is 0.29. The sign of D cannot be determined from the present study. A value of 0.29 for the rhombicity is consistent with the ESR data and gives the best fit to the Mössbauer data with the value for D of 0.85 cm^{-1}, as discussed below.

Mössbauer Spectroscopy. Spectra of solid samples of $[Me_4N][Fe(OEP)O_2]$ embedded in epoxy were recorded at 298, 77, and 4.2 K in the absence of a magnetic field. The species exhibits an intermediate relaxation rate, which leads to a broad spectrum even at 4.2 K. The isomer shift (δ) of 0.67 mm/s, which is observed for $[Me_4N][Fe(OEP)O_2]$, is characteristic of a high-spin ferric state for the iron atom.[22] At room temperature the relaxation rate is not fast enough to allow a direct determination of the magnitude of the quadrupole splitting (ΔE_q), and as a result, this quantity has been treated as a variable in our analysis. The value for ΔE_q obtained from the fit of the low-temperature, high-field spectrum was +0.62 mm/s. The spectrum recorded at 4.2 K in the presence of a 60-kG magnetic field exhibits the typical broad six-line pattern of a high-spin ferric ion, as shown with the theoretical curve in Figure 3. The data have been simulated with a value of 0.85 cm^{-1} for D and a value of 0.29 for λ, which were consistent with the ESR data and gave the best fit to the high-field Mössbauer spectrum. The hyperfine tensor was assumed to be isotropic in these calculations.

(21) Dowsing, R. D.; Gibson, J. F. *J. Chem. Phys.* **1969**, *50*, 294–303.
(22) Lang, G. *Q. Rev. Biophys.* **1970**, *3*, 1–60.

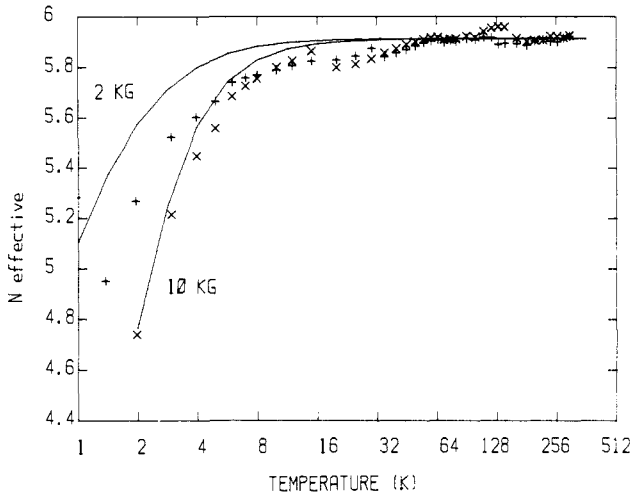

Figure 4. Effective Bohr magneton number, N_{eff}, of $[Me_4N][Fe(OEP)O_2]$ as a function of temperature. The solid curves are calculations based on a $S = {}^5/_2$ spin Hamiltonian with $D = 0.85$ cm^{-1} and $\lambda = 0.29$. The crosses are experimental data taken in an applied field of 2 kG while the X's are experimental data taken in an applied field of 10 kG. Both sets of experimental data are multiplied by 1.036 to bring them into agreement with the calculations at high temperature.

Magnetic Susceptibility Measurements. The temperature dependence of the magnetic moment of $[Me_4N][Fe(OEP)O_2]$ is illustrated in Figure 4. The data conformed to the Curie law from 16 to 300 K. The high-temperature limit of the magnetic moment was 5.75 μ_B, which clearly indicates that the iron atom in this complex is in a high-spin ferric state. A theoretical simulation of the data was carried out with the values of D and λ used to calculate the Mössbauer spectrum. The temperature dependence of the magnetic moment could be modeled for the 10-kG data if the experimental values were multiplied by 1.036 to bring the high-temperature magnetic moment up to the spin-only value. The 2-kG data were observed to deviate from the theoretical curves. This deviation was most pronounced at low temperature where the measured magnetic moment dropped off more rapidly than expected. This type of behavior has been observed in other iron porphyrin systems where it has been attributed to antiferromagnetic coupling between stacked porphyrin molecules.[23] This type of interaction is not expected to occur in $[Me_4N][Fe(OEP)O_2]$ since it is not likely that the charged porphyrin moieties will approach one another. It is reasonable to expect that in this complex the porphyrins will be separated by the tetramethylammonium counterions.

In the case of the iron peroxo complex, the inability of the present Hamiltonian to model completely the susceptibility data reflects the limits of current understanding of the rhombic $S = {}^5/_2$ system. The observation that the effective magnetic moment does not reach the theoretical limit at high temperature is not entirely consistent with the presence of the $g = 4.2$ signal in the ESR spectrum. The low value for the high-temperature magnetic moment, relative to the spin-only value of 5.9 μ_B, could possibly reflect a slight contamination of the sample with the antiferromagnetically coupled μ-oxo ferric porphyrin dimer. We have found no model that would accurately predict both the high- and low-field temperature dependence of the magnetic susceptibility. To the best of our knowledge, there are no high-spin rhombic systems for which the ESR and Mössbauer spectra and the magnetic behavior have been successfully modeled with a single spin Hamiltonian.

Infrared and Visible Spectroscopy. We have previously reported the identification of the peroxide oxygen–oxygen stretch by isotopic substitution in [K18-C-6][Fe(OEP)O_2] in DMSO solution.[5] Figure 5 shows the spectra of the Fe(OEP)O_2^- complex prepared in DMSO in the absence of a potassium chelator and as a solid isolated from CH_3CN with a tetramethylammonium counterion. These spectra are strikingly similar, having distinctive doublets (804, 793 cm^{-1} and 801, 793 cm^{-1}) in the peroxo stretching region. The solution spectrum of the potassium 18-crown-6 salt of Fe(OEP)O_2^- exhibits a single absorption band (806 cm^{-1}), with a small shoulder in the same region.[5] Solutions prepared without a potassium chelator are noticeably less stable than ones prepared in the presence of either 18-crown-6 or kryptand K222, lasting only 0.5 h at room temperature before decomposing. In contrast, solutions of the potassium chelate salts of Fe(OEP)O_2^- remain unchanged for several hours. When either the solid or the solutions of Fe(OEP)O_2^- are exposed to air or allowed to sit for extended periods, the peroxide oxygen stretch disappears and is replaced by new peaks corresponding to the (μ-oxo)ferric porphyrin dimer, $[FeOEP]_2O$.

The visible region of the two iron peroxo complexes, Fe(TPP)O_2^- and Fe(OEP)O_2^-, are shown in Figure 6. The spectral characteristics of these complexes are similar from porphyrin to porphyrin, showing the same features in each system. The energy of the Soret absorption band, the prominent feature in a porphyrin spectrum between 350 and 450 nm, in these complexes is unusually low, and there are pronounced shoulders on the absorption bands

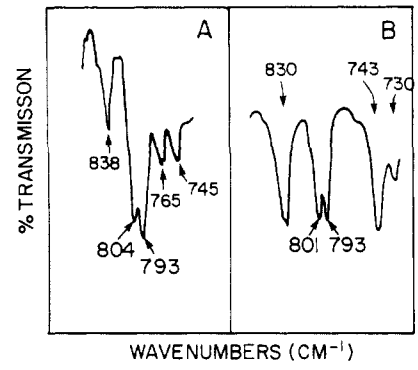

Figure 5. Infrared spectra of the oxygen–oxygen stretching region for (A) [K][Fe(OEP)O_2] in DMSO solution versus a DMSO reference and (B) solid $[Me_4N][Fe(OEP)O_2]$ as a Nujol mull.

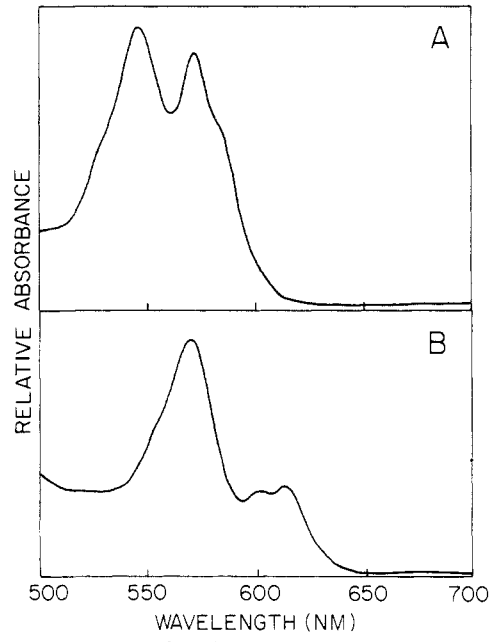

Figure 6. Visible spectra of two iron porphyrin peroxide complexes. Peak positions are given in nm and approximate extinction coefficients in L mol^{-1} cm^{-1}. The extinction coefficients are based on a stoichiometric conversion of the iron porphyrin chloride to the peroxo complex and are therefore only approximate. (A) $[Me_4N][Fe(OEP)O_2]$ in CH_3CN, λ_{max} (ϵ): 530 sh ($6–7 \times 10^3$), 543 (9×10^3), 569 (8×10^3), 582 sh (6×10^3). (B) [KK222][Fe(TPP)O_2] in dimethylacetamide, λ_{max} (ϵ): 552 sh (7×10^3), 567 (1×10^4), 597 (5×10^3), 612 (5×10^3).

(23) Gupta, G. P.; Lang, G.; Scheidt, W. R.; Geiger, D. K.; Reed, C. A. *J. Chem. Phys.* **1986**, *85*, 5212–5220; *J. Chem. Phys.* **1985**, *83*, 5945–5952.

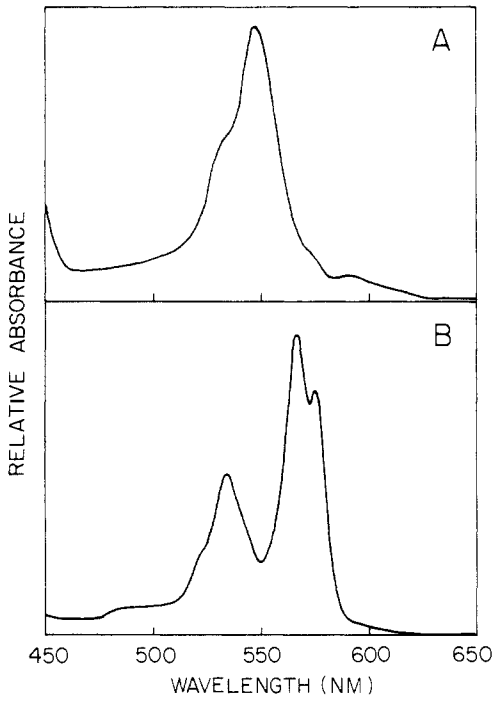

Figure 7. Visible spectra of two titanium porphyrin peroxide complexes. Peak positions are in nm and extinction coefficients in L mol^{-1} cm^{-1}. (A) $Ti(OEP)O_2$ in THF, λ_{max} (ϵ): 575 (2.0×10^4), 565 (2.4×10^4), 533 (1.4×10^4), 520 sh (6.3×10^3). (B) $Ti(TPP)O_2$ in THF, λ_{max} (ϵ): 587 (1.8×10^3), 568 sh (4.5×10^3), 547 (1.9×10^4), 532 sh (1.1×10^4).

between 500 and 700 nm. These characteristics are observed regardless of what counterion is used and in all solvents. The minimal change in the visible spectra when the solvent is changed implies that the solvent does not coordinate to the iron. The related complexes $Ti(TPP)O_2$ and $Ti(OEP)O_2$ also exhibit shoulders on the absorption bands between 500 and 700 nm as illustrated in Figure 7.

Discussion

Most high-spin iron(III) heme complexes are axial as a result of the strong influence of the porphyrin ligand on the iron atom.[24] These complexes are generally five-coordinate, with the iron atom located slightly above the plane of the porphyrin ring. The typical high-spin ferric porphyrin exhibits an axial ESR spectrum with two signals at $g = 6$ and 2.[24] The magnetic susceptibility of these species is characterized by a pronounced non-Curie law temperature dependence below 20 K, which is indicative of a large zero-field splitting.[25] The electronic states of all high-spin ferric species, in the absence of a magnetic field, are described by three sets of Kramers' doublets. In the presence of an axial crystal field, in the case where the zero-field splitting parameter, D, is greater than zero, the energy difference between the lowest two doublets is $2D$ and the energy difference between the middle and upper doublets is $4D$. The magnitude of the zero-field splitting is typically on the order of 10 cm^{-1} for axial high-spin ferric hemes.[25] In these complexes, the lowest Kramers' doublet is isolated from the others by a large zero-field splitting, and therefore the magnetic properties of these complexes arise from this lowest doublet.

$[Me_4N][Fe(OEP)O_2]$ is clearly a high-spin ferric complex as evidenced by the isomer shift of 0.67 mm/s in the Mössbauer spectrum and the high-temperature magnetic moment of 5.75 μ_B, but certain unusual properties have been noted. In their original observations on this complex, Valentine and McCandlish attributed the ESR signal at $g = 4.2$ to a rhombic environment of the ferric ion.[4] Goff was unable to observe NMR signals for the pyrrole protons of the porphyrin ring in the ferric peroxo complex, $Fe(TPP)O_2^-$, due to the extreme relaxation broadening of the protons by the iron atom.[9] The positions of these resonances were determined by deuterium NMR of $Fe(TPP)O_2^-$ prepared from a deuteriated porphyrin and were consistent with the presence of a high-spin ferric heme. The large line widths led the authors to conclude that the zero-field splitting in the iron peroxo complex was unusually small for a high-spin ferric heme. Rhombic ESR spectra and small zero-field splittings are common in simple iron chelates such as $Fe^{III}EDTA(H_2O)$. In this respect, the ligand field of the ferric peroxo complex resembles more closely non-heme ferric complexes where rhombic symmetry is frequently observed.

The solid-state characterization of $[Me_4N][Fe(OEP)O_2]$ was undertaken in order to determine the nature and extent of the rhombicity in this complex and to gain an understanding of how its electronic structure differed from that of other high-spin ferric porphyrins. The iron peroxo complex is unique among high-spin ferric heme complexes because of the high degree of rhombicity it exhibits. High-spin ferric porphyrins with a single sulfur donor ligand are among the few known examples of rhombic high-spin hemes, but typically the rhombic distortion of these complexes is small, with λ less than 0.1. One of the most highly distorted high-spin ferric hemes studied to data is cytochrome P450, which exhibits a rhombicity of 0.1.[24]

The spin Hamiltonian used to describe the electronic states of high-spin rhombic iron is given below.

$$\mathbf{H}_S = g\beta \mathbf{H}\cdot\mathbf{S} + D(S_Z^2 - \tfrac{1}{3}S(S+1)) + E(S_X^2 - S_Y^2)$$

The first term in the spin Hamiltonian is the electronic Zeeman term, which describes the interaction of the electron spin, S, with the external magnetic field, H. The remaining terms are characteristic of the electronic state of the metal atom. The value D is the zero-field splitting parameter, which is related to the energy difference between the Kramer's doublets in the absence of a magnetic field. The value E provides a measure of the rhombicity of the system and can be related to the components of the electron spin orthogonal to the magnetic field. When E is zero, the resulting Hamiltonian is appropriate for an axial ferric system. It is convenient to define a rhombicity parameter, λ, such that $\lambda = E/D$. It has been shown that the value of λ in a completely rhombic field reaches $^1/_3$.[19,26] Such a Hamiltonian is sufficient to model the electron spin resonance and magnetic susceptibility results, but the description of the Mössbauer spectra requires the addition of terms for the nuclear Zeeman interaction and the electron–nuclear hyperfine interaction. This Hamiltonian is given below:

$$\mathbf{H} = \mathbf{H}_S - g_N \beta_N \mathbf{I}\cdot\mathbf{H} + \mathbf{I}\cdot\mathbf{A}\cdot\mathbf{S} + \tfrac{1}{4}QV_{ZZ}\left[I_Z^2 - \tfrac{1}{3}I(I+1) + \tfrac{\eta}{3}(I_X^2 - I_Y^2)\right]$$

Lang has described the origin of the various terms in this Hamiltonian in detail in a review of the Mössbauer spectroscopy of heme proteins.[22] It is sufficient for this discussion to note that both the zero-field splitting parameter, D, and the rhombicity parameter, λ, can be obtained from the measurement and modeling of the Mössbauer spectrum.

The magnetic spectra of the $Fe(OEP)O_2^-$ complex provide information about the degree of rhombicity and the magnitude of the zero-field splitting in this complex. The ESR spectrum provides the primary indication that the structure of the iron peroxo complex is approaching the rhombic limit. The presence of a single absorption at $g = 4.2$ in both the solution and solid spectra is consistent with a high degree of rhombicity. The position and line width of the $g = 4.2$ signal are consistent with $\lambda \geq 0.26$. The simulation of the temperature dependence of the signal intensity was consistent with $0.3 > \lambda > 0.25$. The value of the rhombicity parameter could not be determined independently from the Mössbauer or the magnetic susceptibility, but the good agreement between the experimental data and the theoretical curves obtained, assuming $\lambda = 0.29$, supports the conclusion that

(24) Palmer, G. In *The Porphyrins*; Dolphin, D., Ed.; Academic: New York, 1979; Vol. IV, pp 313–353.
(25) Mitra, S. In *Iron Porphyrins*; Lever, A. B. P., Gray, H. B., Eds., Addison-Wesley: Reading, MA, 1983; Vol. 2, pp 1–42.
(26) Wickman, H. H. Doctoral Dissertation, University of California, Berkeley, 1964.

the ligand field is highly rhombic.

The zero-field splitting parameter, D, has been determined by simulating the Mössbauer spectrum and the temperature dependence of both the ESR signal intensity and the magnetic susceptibility with the Hamiltonian model proposed above. The difference in energy between the two lowest Kramers' doublets was estimated to be 2.9 cm^{-1} from the detailed analysis of the temperature dependence of the $g = 4.2$ ESR absorption, assuming that the rhombicity was close to the theoretical limit. This is consistent with the value of the magnitude of D of 0.85 cm^{-1}, which gives the best fit to the Mössbauer data. This small zero-field splitting is typical of a rhombic iron atom bound to nitrogen and oxygen ligands.[20,27,28] In the rhombic limit, the splitting is between the lower and middle Kramers' doublets and the middle and upper doublets are equivalent and are equal to approximately $3.53D$. Although the spectroscopic data discussed here are insufficient to determine the sign of D, which defines the precise ordering of the Kramers' doublets, the observation that the field is close to the rhombic limit makes the determination of this parameter unnecessary. As the rhombic distortion approaches the theoretical limit, the splitting between the Kramers' doublets becomes symmetrical, and therefore the sign of D is not meaningful.

The spectral characteristics of $Fe(OEP)O_2^-$ may be better understood in light of the structure of the manganese(III) porphyrin peroxide complex $Mn(TPP)O_2^-$[29] since iron and manganese peroxide complexes are expected to be similar. In the $Mn(TPP)O_2^-$ complex, the manganese atom is observed to lie substantially (0.76 Å) above the plane of the porphyrin ring; the influence of the porphyrin on the ligand field of the metal atom is consequently diminished. Charge iterative extended Hückel calculations on the manganese peroxo complex demonstrate that the presence of the peroxide ligand results in a reordering of the orbital energies.[29] In $Mn(TPP)O_2^-$ the d_{z^2} orbital interacts with the peroxide ligand to a lesser extent than the d_{yz} orbital; therefore, the d_{z^2} orbital does not increase in energy as mush as in a more typical metalloporphyrin complex. When the metal is pulled far out of the plane by a strong axial ligand, as in the case of the peroxide dianion, the interaction between the porphyrin nitrogens and the metal is weakened and the $d_{x^2-y^2}$ orbital is lowered in energy. The result of these interactions is the following unusual energy level ordering: $d_{yz} > d_{x^2-y^2} > d_{z^2} > d_{xz} > d_{xy}$.

$Fe(OEP)O_2^-$ may exhibit the unusual geometry and electronic structure observed in the manganese complex. The d_{yz} orbital would be expected to increase in energy as a consequence of the interaction with the dianionic peroxide ligand in this complex, as occurs in the manganese complex. The iron might be expected to lie substantially above the plane of the porphyrin, resulting in a weaker interaction with the porphyrin ligand. This type of geometry could account for the high degree of rhombicity observed in the iron peroxo complex. Such an unusual structure could also account for the absence of multiple electronic transitions in the region between 500 and 700 nm, which are often observed in the visible spectra of ferric porphyrins. These transitions are of considerably greater intensity than typical charge-transfer transitions ($\epsilon \sim 10\,000$ L mol^{-1} cm^{-1}) and are the result of mixing between ligand-to-metal charge-transfer transitions and porphyrin π-π^* transitions. If the iron atom is substantially out of the plane, the porphyrin π orbitals would not be expected to overlap well with the metal d orbitals; therefore, the extra visible transitions would not be observed.

The ferric porphyrin peroxide complexes exhibit two other unusual features in their visible spectra: an unusually low-energy Soret band and an apparent splitting of the two absorptions in the region between 500 and 700 nm. The red-shifted Soret absorption, occurring at 438 nm in $Fe(TPP)O_2^-$ and at 418 nm in $Fe(OEP)O_2^-$, led early investigators to conclude that this complex was a ferrous species.[30] The Soret band in ferrous porphyrins is typically 10–20 nm higher than the corresponding absorption in ferric complexes.[31] The magnetic characterization of the iron peroxide complex presented here, however, clearly indicates that the iron is in the ferric oxidation state; therefore, the lower energy of the Soret transition must have a different origin in this system. Nappa and Valentine[32] correlated the position of the optical absorption bands in the spectra of zinc porphyrins with the charge and polarizability of the axial ligand. A greater negative charge on the ligand led to a decrease in the energy of the transitions. On this basis, the presence of a dianionic ligand, such as a peroxide, is likely to cause a substantial decrease in the transition energy. The Soret absorption of the manganese porphyrin peroxide complex also occurs at lower energy than is common for manganese(III) porphyrins, which supports the suggestion that this shift in Soret frequency is a function of the peroxide ligand.

The second unique feature of the visible spectra of the ferric porphyrin peroxide complexes is the splitting of the two absorptions that occur between 500 and 700 nm. This feature is also observed in the visible spectra of titanium(IV) porphyrin peroxide complexes as shown in Figure 7. We postulate that this splitting arises from the lowering of the symmetry of the porphyrin complex in the presence of the bound peroxide ligand. The free base porphyrin, which has D_{2h} symmetry due to the presence of the protons on two of the nitrogen atoms, has four bands in the region from 500 to 700 nm. Introduction of a metal into the ring increases the symmetry to D_{4h}, and only two absorption bands are normally observed in this region. The presence of axial ligands does not typically disrupt the fourfold symmetry of the porphyrin ring, and as a result two transitions are observed for most metalloporphyrin complexes. Crystal structures of the $Ti^{IV}(OEP)O_2$,[33] the $Mo^{VI}(TTP)(O_2)_2$,[34] and the $Mn^{III}(TPP)O_2^-$[29] metalloporphyrin peroxides all show that the peroxide ligand eclipses two of the metal–nitrogen bonds and therefore lowers the symmetry of the complex. The molecular symmetry of the monoperoxide complexes is therefore C_{2v}, and this lower symmetry may be the source of the splitting of the absorption bands.

The observation that the peroxide oxygen–oxygen stretching mode in the infrared spectrum splits into a doublet in the absence of a potassium chelating agent suggests that there are two populations of peroxide ligands. In the previous report on $Fe(OEP)O_2^-$,[5] it was noted that even in the presence of a chelating agent a shoulder was observed at 796 cm^{-1} on the 806-cm^{-1} peak that shifted with isotopic substitution. In the absence of 18-crown-6, the peroxide stretch was observed to split into two peaks of approximately equal intensity (804 and 793 cm^{-1}). The same splitting of the peroxide stretch was observed in the solid state with a tetramethylammonium counterion. The presence of the potassium chelators alters the relative intensities of the two bands, which suggests that this phenomenon may be an ion-pairing effect. The larger potassium 18-crown-6 cation would be less likely to interact strongly with the peroxide ligand because of steric hinderance between the chelated ion and the porphyrin ring. The free potassium or tetramethylammonium cations, however, are small enough to approach the negatively charged peroxide ligand and form specific ionic interactions with one of the oxygen atoms.

Conclusions

The solid-state characterization of the ferric porphyrin peroxide complex, $[Me_4N][Fe(OEP)O_2]$, provides the first detailed study of a rhombic high-spin ferric porphyrin complex. The iron atom is in the high-spin ferric oxidation state, as confirmed by the

(27) Peisach, J.; Blumberg, W. E.; Lode, E. T.; Coon, M. J. *J. Biol. Chem.* **1971**, *246*, 5877–5811.
(28) Que, L.; Lipscomb, J. D.; Zimmerman, R.; Munck, E.; Orme-Johnson, N. R.; Orme-Johnson, W. H. *Biochim. Biophys. Acta* **1976**, *452*, 320–334.
(29) Van Atta, R. B.; Strouse, C. E.; Hanson, L. K.; Valentine, J. S. *J. Am. Chem. Soc.* **1987**, *109*, 1425–1434.
(30) Afanas'ev, I. B.; Prigoda, S. V.; Khenkin, A. M.; Shteinman, A. A. *Dokl. Akad. Nauk SSSR* **1977**, *236*, 641–644; English translation, pp 902–905.
(31) Adar, F. In *The Porphyrins*; Dolphin, D., Ed. Academic: New York, 1978; Vol. III, pp 167–209.
(32) Nappa, M.; Valentine, J. S. *J. Am. Chem. Soc.* **1978**, *100*, 5075–5080.
(33) Guilard, R.; Latour, J.-M.; Lecomte, C.; Marchon, J.-C.; Protas, J.; Ripoll, D. *Inorg. Chem.* **1978**, *17*, 1228–1237.
(34) Chevrier, B.; Diebold, Th.; Weiss, R. *Inorg. Chim. Acta* **1976**, *19*, L57–L58.

magnetic susceptibility, ESR, and Mössbauer spectra, but unlike other high-spin ferric hemes, this complex is rhombic. The uncommon spectral characteristics of this complex are attributed to the presence of the peroxide ligand. While it is not possible to determine the geometry of the $Fe(OEP)O_2^-$ complex conclusively without a crystal structure, the magnetic spectra suggest that the iron peroxide complex may have a geometry similar to that of the manganese(III) porphyrin peroxide, $Mn(TPP)O_2^-$, where the metal ion is significantly displaced out of the plane of the porphyrin toward the peroxo ligand. In fact, the EXAFS data measured of the ferric complex, $[Na(THF)_3][Fe(TPP)O_2]$, and reported by Friant et al.[13] are consistent with the displacement of the iron from the plane of the porphyrin. Measurements of the rhombicity and the zero-field splitting in $Fe(OEP)O_2^-$ are consistent with the geometry proposed.

Acknowledgment. We thank Dr. Charles E. Strouse (UCLA) for helpful discussions. Dr. Jean-Marc Latour (CNRS, Grenoble, France) generously provided samples of the titanium peroxide complexes. This work was supported by grants from the National Science Foundation (J.S.V.) and the National Institutes of Health (G.L.; HL-16860).

Registry No. $[Me_4N][Fe(OEP)O_2]$, 112421-74-6; Fe(OEP)Cl, 28755-93-3.

Second-Order Perturbation Theory and Configuration Interaction Theory Applied to Medium-Sized Molecules: Cyclopropane, Ethylenimine, Ethylene Oxide, Fluoroethane, and Acetaldehyde

Emmanuel D. Simandiras,[†] Roger D. Amos,[†] Nicholas C. Handy,[†] Timothy J. Lee,[‡,§] Julia E. Rice,[‡,§] Richard B. Remington,[‡] and Henry F. Schaefer III*[‡]

Contribution from the University Chemical Laboratory, Lensfield Road, Cambridge CB2 1EW, England, and Department of Chemistry, University of California, Berkeley, California 94720.
Received May 4, 1987

Abstract: A systematic comparison of post Hartree–Fock theoretical predictions for molecular structures and vibrational frequencies has been undertaken for the five species identified in the title. Double-ζ plus polarization (DZP) basis sets are used throughout, and for ethylenimine, a significantly larger basis set is used (in addition) to address an inconsistency with respect to experiment. Although good agreement with available experiments is generally reported, a revised assignment of the C_2H_4NH vibrational frequencies is suggested. Theory also allows a clear choice between two existing experimental assignments of the fluoroethane vibrational frequencies.

1. Introduction

It is now increasingly common for ab initio studies on small molecules (defined perhaps as containing two heavy atoms or less) to be considered as worthy of publication only if an attempt has been made to include electron correlation effects. We suggest that the time is quickly approaching when the same situations will hold for medium-sized systems.

There are two commonly used methods for the inclusion of electron correlation that are applicable to the larger systems, compatible with the use of good basis sets. The simplest of these methods, based on second-order perturbation theory, is commonly called MP2.[1] The other approach is based on the variational principle and is called CISD,[2] configuration interaction including all single and double replacements from the self-consistent-field reference function. MP2 has indeed been applied to rather large molecular systems;[3] full geometrical optimizations and force constant analyses have been performed for molecules as large as malonaldehyde.[4] CISD programs are more complicated, and as such there is not yet available the wealth of evidence for this approach. We suspect that the largest molecules (in terms of both the number of atoms and the number of unique geometrical parameters) for which full CISD geometry optimizations and vibrational analyses have been performed are the hydrogen-bonded complex $H_5O_2^+$[5a] and bicyclobutene, a C_4H_4 isomer.[5b]

Recent advances in gradient theory have enabled our research groups to develop efficient computer programs for the evaluation of MP2 and CISD energies and their gradients.[6] We contend that it is now appropriate to study a series of medium-sized molecules, with good basis sets, by both methods, so that the results may be compared for their reliability.

Let us briefly comment on advantages and disadvantages of these two methods. MP2 has the advantage that it is very simple and also size extensive. It has the disadvantage that it is only applicable to closed-shell systems or open-shell systems, which are well represented by the unrestricted Hartree–Fock (UHF) determinant. Alternatively, CISD is a fully variational procedure, operating in space and spin symmetry, but truncated CI expansions are not size extensive. Both methods are dependent upon the dominance of the reference configuration, but CISD is less so

[†] University Chemical Laboratory.
[‡] University of California.
[§] Present address: University Chemical Laboratory, Lensfield Rd., Cambridge CB2 1EW, England.

(1) Møller, C.; Plesset, M. S. *Phys. Rev.* **1934**, *46*, 618.
(2) E.g.: Roos, B. O.; *Chem. Phys. Lett.* **1972**, *15*, 153.
(3) See: Hehre, W. J.; Radom, L.; Schleyer, P. v. R.; Pople, J. A. *Ab Initio Molecular Orbital Theory*; Wiley: New York, 1986.
(4) Binkley, J. S.; Frisch, M. J.; Schaefer, H. F. *Chem. Phys. Lett.* **1986**, *126*, 1.
(5) (a) Remington, R.; Schaefer, H. F. Presented at the American Chemical Society National Meeting, Miami Beach, May 1, 1985; Symposium on Gas Phase Ions, Division of Physical Chemistry, Abstract 103. (b) Hess, B. A.; Allen, W. D.; Michalska, D.; Schaad, L. J.; Schaefer, H. F. *J. Am. Chem. Soc.*, in press.
(6) (a) Handy, N. C.; Amos, R. D.; Gaw, J. F.; Rice, J. E.; Simandiras, E. D. *Chem. Phys. Lett.* **1985**, *120*, 151. (b) Rice, J. E.; Amos, R. D.; Handy, N. C.; Lee, T. J.; Schaefer, H. F. *J. Chem. Phys.* **1986**, *85*, 963.

0002-7863/88/1510-1388$01.50/0